NATIONAL ADVISORY COMMITTEE FOR AERONAUTICS

TECHNICAL NOTE

No. 997

PERFORMANCE TESTS OF WIRE STRAIN GAGES

III - CALIBRATIONS AT HIGH TENSILE STRAINS

By William R. Campbell
National Bureau of Standards

Washington
December 1945

NATIONAL ADVISORY COMMITTEE FOR AERONAUTICS

TECHNICAL NOTE NO. 997

PERFORMANCE TESTS OF WIRE STRAIN GAGES

III – CALIBRATIONS AT HIGH TENSILE STRAINS

By William R. Campbell

SUMMARY

Results of calibrations in axial tension over the strain range 0 to 0.03 are presented for 15 types of single element, multistrand wire strain gages. The relation between change in resistance and strain showed deviations from linearity to a strain of about 0.01 which were of the same order as the deviations previously found in tensile calibrations at low strains. At higher strains the curve of change in resistance versus strain in many cases approached a straight line having lower slope than the initial slope. Gages failed by rupture of the wire strands in 58 percent of the calibrations. Measurements for decreasing strain after an applied strain of 0.03 indicated hysteresis in all cases. The strains computed from the measured changes in resistance of gages of types A, C-1, D, and F, using the average calibration factors for low tensile strains, differed less than 5 percent from the measured strains up to a strain of 0.03.

INTRODUCTION

This report describes part of a series of performance tests on wire strain gages of types currently used in large numbers to measure stresses in aircraft structures. The purpose of the tests is to make available information on the properties, accuracy, and limitations of various multistrand, single element gages.

The performance test program has been divided into several phases the results of which are being reported individually. The first two phases of the program, calibration factors in tension and in compression for low strains, have been

reported in references 1 and 2, respectively. The present paper reports on the third phase, calibrations under axial tension at strains between 0 and 0.030. The performance tests that remain to be made are to include measurements of the effects of temperature, humidity, finite gage width in the presence of transverse stress, and thickness and rigidity of gage.

The performance tests on wire strain gages are being conducted at the National Bureau of Standards under the sponsorship of the National Advisory Committee for Aeronautics.

NOTATION

ϵ axial strain

$\Delta\epsilon$ change in axial strain

μ Poisson's ratio

K calibration factor of wire strain gage for uniaxial stress producing a change in strain $\Delta\epsilon$ parallel to the gage axis and a strain $-\mu\Delta\epsilon$ transverse to the gage axis

R gage resistance, ohms

ΔR change in gage resistance due to change in strain $\Delta\epsilon$, ohms

K_{mt} average calibration factor K for eight gages of a given type at low tensile strains (Computed from table 2 of reference 1 as the average of 16 factors, 8 for strain increasing and 8 for strain decreasing)

APPARATUS AND METHOD

Description of Strain Gages

Six aircraft companies, the Ames Aeronautical Laboratory of the NACA, the Baldwin Locomotive Works, and the Chrysler Corporation contributed test gages of 15 different types (A, B, C-1, D, E, F, G, H-1, I, J, K, L, M, N, O) which in all

but two cases are identical with the gage types reported in reference 1. With the exception of gage types C-1 and H-1, which were substituted by the makers for gage types C and H, table 1 of reference 1 gives a description of the test gages and figures 1 and 2 of reference 1 show the gages attached to test strips used in the calibrations at low tensile strains. Data on gage type C-1 are given in appendix 1 of this report and data on gage type H-1 are given in appendix 1 of reference 2.

Attachment of Gages

All gages were attached at the National Bureau of Standards to 18- by 1- by 0.125-inch 24S-T aluminum-alloy calibration strips as shown in figure 1. Samples of bonding cements for various gages were supplied by the makers and all gages were attached following the maker's instructions. All gages were dried a minimum of 40 hours at room temperature. No gages were dried at elevated temperatures, and no gages were waterproofed.

Calibrations

The gages were calibrated by measuring changes in gage resistance ΔR corresponding to known changes in strain $\Delta\epsilon$. The calibration factor K is commonly defined as

$$K = \frac{\Delta R}{R} \frac{1}{\Delta\epsilon} \qquad (1)$$

The changes in resistance ΔR were measured for strains between 5×10^{-4} and 300×10^{-4}. The lower strain limit corresponded to the initial load used to aline the test strip in the testing machine. The upper strain limit of 300×10^{-4} was the maximum strain that could be obtained, without resets, with the Tuckerman strain gage used to measure calibrating strains. An upper limit of 300×10^{-4} was considered adequate since it is equal to several times the yield strain of metals used in aircraft.

It should be noted that the calibration factor defined by equation (1) remains constant only as long as Poisson's ratio remains constant. Since Poisson's ratio for aluminum alloy changes from about 0.3 in the elastic range to about

0.5 in the plastic range, there will be a corresponding change in calibration factor. It is shown in appendix 2 that this change in calibration factor is of the order of −0.01 or −0.5 percent for a gage having a calibration factor of 2.00.

Strain Measurements

The calibrating strain applied to each wire gage was measured with a Tuckerman optical strain gage having a 1.0-inch lozenge and a 2-inch gage length (fig. 1).

Resistance Measurements

The method of measuring resistance changes at large tensile strains had to be changed from that used for calibrations at low tensile strains (reference 1), where an exceptionally accurate ratio set and a sensitive galvanometer were used. At large tensile strains there was a likelihood of rupture of gage wires during calibration, leading to excessive galvanometer current and probable damage to the galvanometer suspension. Furthermore, the range of resistance changes to be measured was in all cases greater than the range provided for in the ratio set. These two difficulties were overcome, without too much sacrifice in accuracy, by measuring the change in resistance with a Rubicon resistance decade box in an alternating current Wheatstone bridge, and using a cathode ray oscillograph as null indicator. The decade box provided an adequate range of change in resistance and the cathode ray oscillograph provided an indicator that was not damaged by a sudden open circuit in one arm of the bridge.

A diagram of the Wheatstone bridge and indicating circuit used for the calibrations is shown in figure 2. The A-arm of the bridge represents the calibrating arm and includes the test gage; the B-arm represents the compensating arm and includes a dummy gage of the same type as the test gage. Inserted in the A and B arms in series with test gage and the dummy gage were two Rubicon resistance decade boxes C and D. Decade C, in series with the test gage, was used to measure both gage resistance R and change in gage resistance ΔR due to applied strain. The quantity $-\Delta R$ was measured as the change in resistance of C required to restore balance after applying a known change in strain to the test gage. The arms E and F of the bridge represent the two 1000-ohm arms of a Campbell-Shackelton shielded a-c ratio box (reference 3). The ratio box has a nominally fixed ratio

between the two arms E and F of 1:1 and incorporates controls for small adjustments in both resistive and reactive balance components. The box is thoroughly shielded and for any given setting provides a stable ratio which is negligibly affected by stray electrostatic fields. Reactive balance of the complete bridge ABEF was maintained within the adjustable range of the ratio box by making the arms A and B as near as possible electrically symmetrical.

The input signal to the bridge was supplied by an audio oscillator delivering approximately 2 volts at 1500 cps . The bridge output due to resistive or reactive unbalance was amplified and filtered with a 1500-cps band-pass filter, and the filtered signal was impressed on the horizontal plates of a 5-inch cathode ray oscillograph. Amplifier and oscillograph gains were adjusted to provide a bridge sensitivity equal to the least count of the Tuckerman strain gage, so that a change in strain at the test gage of 5×10^{-6} produced a readily detectable oscillograph deflection. The laboratory setup for resistance measurements is shown in figure 3.

The maximum total change in resistance ΔR anticipated at the test gage during calibrations was estimated for the purpose of providing range on decade C by solving equation (1) for ΔR,

$$\Delta R = KR(\Delta\epsilon) \tag{2}$$

and substituting the maximum values, those for gage type N:R = 500 ohms, K = 3.5; and the maximum strain desired, $\epsilon = \Delta\epsilon = 0.03$, giving,

$$\begin{aligned} \Delta R &= 3.5 \times 500 \times 0.03 \\ &= 52.5 \text{ ohms} \end{aligned} \tag{3}$$

The anticipated change in resistance ΔR for a strain of 0.03 was calculated for each gage as in equations (2) and (3) and divided into convenient increments which could be successively subtracted from the initial resistance set on decade C. These increments were used to unbalance the bridge by known amounts $-\Delta R$. Balance was restored by straining the test gage in tension to produce a resistance change $+\Delta R$, which increased the resistance of the A-arm to its initial value.

TEST PROCEDURE

Two gages of each type were calibrated, and if one or both of these gages failed at a strain less than 0.03, a third gage was calibrated.

The same test procedure was followed in calibrating all gages. The calibration strip G (fig. 4) with one wire strain gage attached was mounted in Templin grips in a 60,000-pound testing machine under an initial load of 200 to 500 pounds. The Tuckerman strain gage H was mounted on the strip so as to span the wire gage and, when clearances permitted, contact the strip at points equidistant from the transverse center line of the wire gage grid. A second calibration strip J, upon which was attached a dummy gage of the same type as the test gage, was clamped at one end in a grip suspended from the upper head of the testing machine.

With decade D (fig. 2), in series with the dummy gage, set at 75.0 ohms (>52.5 ohms), the bridge was balanced by adjusting decade C first with the leads to the test gage disconnected and shorted and then again with the test gage connected. On this balance the initial load on the calibration strip was adjusted to bring the bridge to exact balance. The difference between the two settings of decade C was taken as the resistance R of the test gage. With the bridge initially balanced, the procedure for calibration was similar to that described in references 1 and 2. Known resistance changes were set on the dials of decade C in the A-arm of the bridge; the load on the calibration strip was increased until the change in resistance of the wire gage rebalanced the bridge; and the strain at the instant of balance was measured with the Tuckerman strain gage. The load was increased until the strain at the gage was 0.03, after which the load was reduced to about 500 pounds and $\Delta R/R$ and strain were measured again to determine the accuracy of the wire gage in measuring permanent set.

The average strain rate during calibrations was of the order of 3×10^{-4} per minute. Between readings the strain rate was about 5×10^{-4}, while during readings the rate was nearer 1×10^{-4}. Reactive balance of the bridge was maintained by adjusting the variable condenser of the ratio box to obtain a minimum oscillograph deflection immediately following the minimum deflection or "dip" produced by the changing gage resistance.

ACCURACY

The accuracy of the calibrations is limited by the errors in the measurements of gage resistance R, change in resistance ΔR, and change in strain $\Delta\epsilon$.

The decade resistance box used for measuring both R and ΔR was guaranteed by the makers to have a maximum error not greater than ± 0.1 percent for resistances greater than 1 ohm. The resistances of the 0.1-ohm coils were guaranteed to be within ± 0.25 percent of their nominal values. Calibration of the decade for changes in resistance showed the combined errors due to variations in switch resistance and to deviations of the 0.1-ohm coils from their nominal values to be less than 0.001 ohm, or 1 percent of the smallest increment of the resistance box. It was estimated that the limiting error in the measurement of $\Delta R/R$ was therefore of the order of 0.3 percent for changes in resistance greater than 1 ohm.

The error in the measurement of change in strain is due almost entirely to nonuniform yielding of the calibration strip within the Tuckerman gage length. A survey made on a strip with two 1-inch Tuckerman gages on adjacent gage lengths showed that the average strains for the two gage lengths differed by as much as ± 1 percent for strains greater than 0.01. The difference between the average strain over the grid of the wire gage and the average strain measured by the 2-inch Tuckerman gage during calibrations was assumed to be of the same order (± 1 percent). The accepted accuracy of the Tuckerman gage itself is ± 0.1 percent, which contributes considerably less error than that due to nonuniform yielding of the test strip.

Combining the errors in the measurements of both resistance and strain, it was estimated that the total error in the measured deviations was less than 1.5 percent.

RESULTS

Calibrations were made on 43 gages, of which 25 gages, or 58 percent, failed prior to sustaining a strain of 0.03. No attempt was made to determine calibration factors for the whole range of strain in view of the large nonlinearities found in most calibrations at high tensile strains. It

seemed more useful to compare applied strains with strains indicated by the wire gages using calibration factors determined at relatively low tensile strains. Such a comparison would bring out directly the errors involved in basing strain measurements beyond the elastic range on calibrations inside the elastic range.

Table 1 gives the average calibration factors in tension K_{mt} for each type of gage at low tensile strains, $\epsilon_{max} = 0.002$. The value of K_{mt} is the average of the 16 factors given for each gage type in table 2 of reference 1. Indicated strains were computed by substituting the measured values of $\Delta R/R$ and $K = K_{mt}$ in

$$\text{indicated strain} = \frac{1}{K_{mt}} \frac{\Delta R}{R} \tag{4}$$

Table 2 gives the strains at which the indicated strain differed from the applied strain, as measured by the Tuckerman gage, by ± 2, ± 5, and ± 10 percent of the applied strain. The difference between the permanent set in the calibration strip as determined by the Tuckerman gage and that indicated by the wire gages using equation (4) is given in table 2 as a percentage of the set strain measured by the Tuckerman gage. Set readings were obtained on only those gages which sustained the maximum calibrating strain of 0.03. Table 2 also gives the maximum strain applied to each gage and the type of failure.

Calibration curves $\Delta R/R$ versus ϵ and deviation curves $\Delta R/R$ versus $\epsilon - (\Delta R/R)/K_{mt}$ are given in figures 5 to 19. The deviation curves indicate the nature of nonlinearities in the calibration curves by magnifying the deviation of the indicated strains from those given by a straight line through the origin with slope K_{mt}. Departure of the calibration factors from the average, K_{mt}, for low strains is indicated by the slope of the deviation curve relative to the vertical axis. A factor lower than K_{mt} is indicated by a slope to the right, and a factor greater than K_{mt} by a slope to the left. Hysteresis is indicated by a displacement of the "set" point to the right of the remainder of the calibration curve and the deviation curve.

DISCUSSION

The calibrations at high tensile strains, just as those at low strains reported in references 1 and 2, have several characteristics which, in varying degrees, are common to all the gages tested. Inspection of the curves of figures 5 to 19 shows that in every calibration the calibration factor decreased for increasing strains as indicated by deviations to the right of the vertical axis. The minimum reduction in factor at high strains was observed with gage type D, which showed the average calibration factor for strains between 0.01 and 0.03 to be about 2 percent lower than the average factor K_{mt} at low strains. Gages of types A, C-1, D, and F were observed to have reductions of about 5 percent or less.

Examination of the data for low strains in figures 5 to 19 showed good agreement with the deviation curves for low strains in reference 1. The deviation curves showed considerable nonlinearity at strains between 0.0025 and 0.006. In many cases there was an improvement in linearity, with a reduced calibration factor, at strains greater than 0.01.

Tabulation of the number of gage failures occurring in the calibrations showed that 25 gages out of 43 or 58 percent failed before reaching a strain of 0.03. Failure was caused by parting of the strain-sensitive wire at or within about 0.05 inch of an internal solder joint in 84 percent of the cases. The remaining failures involved breaks in the leading wire strand at points more than 0.05 inch from the solder joint. In view of the high percentage of failures near the soldered joints, it seems desirable that gages for measuring high strains be designed for attachment without cementing the soldered joints. Gages of type C-1 (fig. 20) were so designed, and all of them sustained the maximum strain of 0.03 without failure. Breaking of the strain-sensitive wire was, in most cases, preceded by a sharp increase in $\Delta R/R$ for small changes in strain, as best illustrated in figures 10, 15, and 19. The deviation curve under this condition shows extremely large deviations to the left (negative) since the second term $(\Delta R/R)/K_{mt}$ in the expression for the deviation $\epsilon - (\Delta R/R)/K_{mt}$ rapidly exceeds the calibrating strain ϵ due to the increase in $\Delta R/R$. In only two cases (figs. 14 and 19), both of which involved a fast-drying, celluloid-ethyl acetate cement, was failure of the wire preceded by a decrease in $\Delta R/R$, indicating a

failure of the bonding cement to transfer strain. Because of this, $(\Delta R/R)/K_{mt}$ becomes smaller than ϵ and the deviation curve is deflected to the right.

Examination of figures 5, 7, 8, 10, 13, 14, and 17 shows that the "set" point was, in every case, on the right side of the curve, indicating a certain amount of hysteresis in the gages. The dotted line connecting the point for the highest strain with the "set" point was nearly vertical on the deviation curves. It may be concluded that the strain indicated by the wire gages for decreasing strain can be computed with the calibration factor for low strain even after subjecting the gages to tensile strains as high as 0.03. This conclusion may be expressed in another way by saying that the error in the measurement of permanent set is caused principally by deviations of the calibration factor from the value K_{mt}, for increasing strain. Table 2 shows that the minimum error of 1 percent in the measurement of set strain was obtained with a gage of type D.

CONCLUSIONS

The deviation curves showed considerable nonlinearity at strains between 0.0025 and 0.006. In many cases there was an improvement in linearity with reduced calibration factor at strains greater than 0.01. The calibration factor for decreasing strain was nearly equal to that for low strains even after subjecting the gage to tensile strains as high as 0.03. Fifty-eight percent of the gages failed by breaking of the strain-sensitive wire at strains less than 0.03.

The strain indicated by gages of types A, C-1, D, and F, using the calibration factors for small strains, differed less than 5 percent from the applied strains for strains up to 0.03.

National Bureau of Standards,
Washington, D. C., March 5, 1945.

APPENDIX 1

DESCRIPTION OF GAGE C-1

Gage C-1 was substituted by the maker for gage type C. Gage C-1 (fig. 20) is intended for use in measuring large strains and differs from gage C in that the internal solder connections to the strain-sensitive wire grid are further removed from the grid than in gage C. Only the grid and a short length of the leading or outside wire strands are cemented to the structure, leaving the gage area in the vicinity of the solder joints uncemented. The gage has a slightly higher resistance than gage C due to the additional length of strain-sensitive wire, and a somewhat lower calibration factor than gage C because the uncemented wire does not contribute to the output of the gage. The following data on gage C-1 are given to supplement table 1 of reference 1 on "Description of Gages."

Gage type	Nominal dimensions		Approximate length of grid	Wire material	Cement	Type of winding	Nominal resistance
	Length (in.)	Width (in.)	(in.)				(ohms)
C-1	2.3	0.04	1.00	--------	Duco	Grid	95

APPENDIX 2

CHANGE IN CALIBRATION FACTOR WITH CHANGE IN POISSON'S RATIO

The calibration factor defined by equation (1) is constant only as long as Poisson's ratio remains constant. The calibration factor K is related to Poisson's ratio by

$$K = K_L - \mu K_T \tag{5}$$

where

K_L longitudinal sensitivity of wire gage for zero transverse strain

K_T transverse sensitivity of wire gage for zero longitudinal strain

The change in K for a change in μ equal to $\Delta\mu$ is

$$\Delta K = -K_T \Delta\mu \tag{6}$$

Assuming 0.05 as a reasonable value for K_T, the change in calibration factor ΔK for a change in Poisson's ratio of 0.2 is given by (6) as,

$$\begin{aligned} \Delta K &= -0.05\ (0.2) \\ &= -0.01 \end{aligned} \tag{7}$$

Equation (7) indicates that, due to the change in Poisson's ratio from 0.3 in the elastic range to about 0.5 in the plastic range, the calibration factor may be expected to decrease about 0.01 or 0.5 percent for a gage having a calibration factor of 2.00.

REFERENCES

1. Campbell, William R.: Performance Tests of Wire Strain Gages. I – Calibration Factors in Tension. NACA TN No. 954, 1944.

2. Campbell, William R.: Performance Tests of Wire Strain Gages. II – Calibration Factors in Compression. NACA TN No. 978, 1945.

3. Behr and Williams: The Campbell-Shackelton Shielded Ratio Box. Proc. I.R.E., June 1932.

TABLE 1.- AVERAGE CALIBRATION FACTORS FOR LOW TENSILE STRAINS ($\epsilon_{max} = 0.002$)

Gage type	K_{mt}	Gage type	K_{mt}
A	[a]2.027	I	[a]2.149
B	[a]2.083	J	[a]2.088
C-1	[b]1.90	K	[a]2.170
D	[a]2.058	L	[a]2.243
E	[a]2.104	M	[a]1.980
F	[a]2.037	N	[a]3.480
G	[a]2.314	O	[a]2.086
H-1	[c]1.990		

[a]Computed from table 2 of reference 1 as the average of 16 calibration factors for each type of gage.

[b]No low-strain tensile calibrations were obtained on gage C-1, a special gage for use at high strains. The value given for K_{mt} (1.90) is the estimated average limiting slope of the calibration curves given in fig. 7 as the strain approaches zero.

[c]No low-strain tensile calibrations were obtained on gage H-1. Owing to good agreement between the average tension and average compression calibration factors for most gages at low strains, the average low strain compression factor $K_{mc} = 1.990$ is used here.

TABLE 2.- RESULTS OF TESTS

Gage type	Gage number	Maximum strains[a] at which gage is in error by less than ±2 percent	±5 percent	±10 percent	Maximum strain applied	Error in set measurement[a] as percentage of set strain	Remarks on failure
		$\epsilon \times 10^4$	$\epsilon \times 10^4$	$\epsilon \times 10^4$	$\epsilon \times 10^4$	percent	
A	1	38	> 300	----	301	6	-------
	2	125	> 300	----	308	5	-------
B	1	15	52	> 102	102	-------	(b)
	2	29	70	176	243	-------	(b)
	3	44	85	> 190	190	-------	(b)
C-1	1	45	292	> 303	303	7	-------
	2	50	> 299	----	299	5	-------
	3	65	> 299	----	301	5	-------
D	1	60	> 308	----	308	3	-------
	2	60	> 310	----	310	1	-------
E	1	54	106	> 113	113	-------	(c)
	2	25	75	> 75	75	-------	(c)
	3	12	25	92	204	-------	(b)
F	1	< 12	212	213	213	-------	(c)
	2	12	64	> 307	307	6	-------
	3	12	64	> 306	306	5	-------
G	1	----	----	< 12	82	-------	(c)
	2	< 12	12	30	108	-------	(c)
	3	< 12	12	47	73	-------	(c)
H-1	1	25	72	120	225	-------	(c)
	2	13	33	84	83	-------	(c)
	3	25	77	> 106	106	-------	(c)
I	1	25	60	230	304	13	-------
	2	25	98	> 309	309	12	-------
	3	25	61	271	298	13	-------
J	1	26	292	> 310	310	7	-------
	2	26	250	> 252	252	-------	(c)
	3	32	220	240	265	-------	(c),(d)
K	1	20	50	154	218	-------	(c)
	2	20	61	195	296	-------	(c)
	3	22	30	165	188	-------	(c)
L	1	23	46	70	301	27	-------
	2	23	35	62	312	30	-------
	3	40	55	81	310	28	-------
M	1	< 15	< 15	53	241	-------	(c)
	2	< 15	26	69	309	21	-------
	3	< 15	26	69	292	20	-------
N	1	54	70	100	131	-------	(c)
	2	54	70	100	112	-------	(c)
	3	54	70	100	103	-------	(c)
O	1	15	> 287	----	287	-------	(c)
	2	15	244	246	246	-------	(c)
	3	15	195	> 241	241	-------	(c),(d)

[a] Strain indicated by wire gage = $(\Delta R/R)/K_{mt}$.

[b] Break in leading wire strand (edge of grid) 0.05 in. or more from solder joint.

[c] Break in leading wire strand at or within 0.05 in. of solder joint.

[d] Evidence of failure in cement.

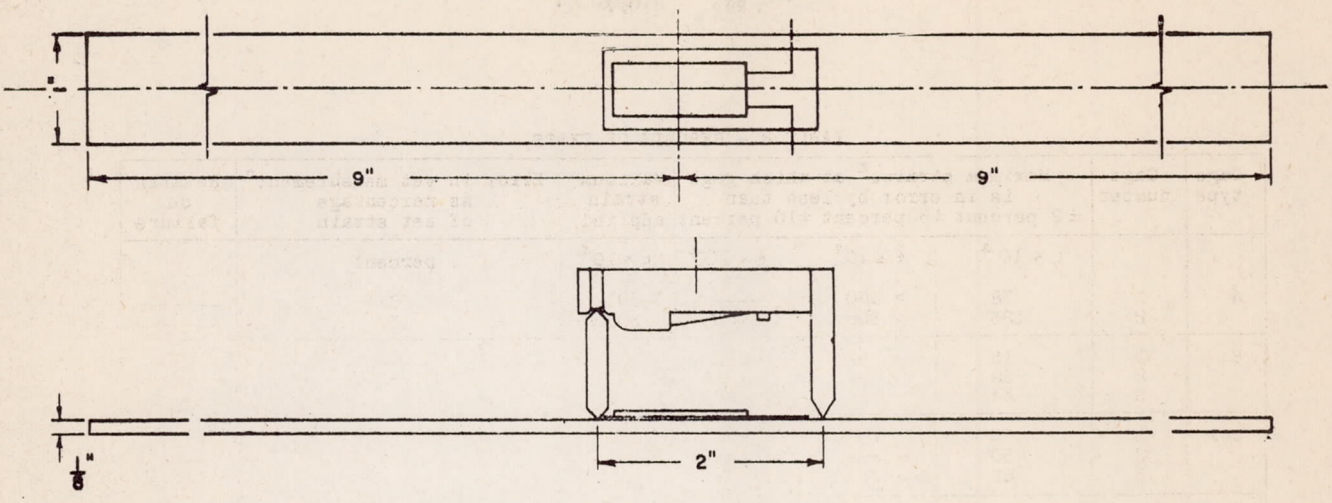

Figure 1.- Location of wire strain gage on calibration strip and position of Tuckerman gage during calibrations.

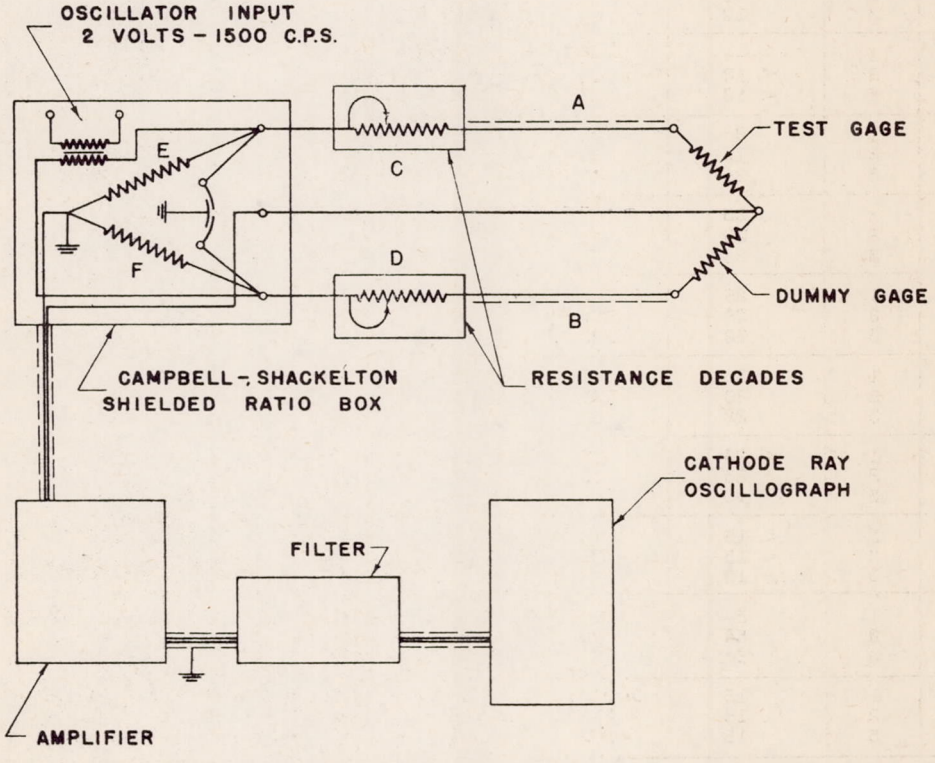

Figure 2.- Circuit for resistance measurements. Resistance decade C was used to provide known changes $-\Delta R$ which were in turn compensated by changes $+\Delta R$ at the test gage by changes in calibrating strain $\Delta\epsilon$.

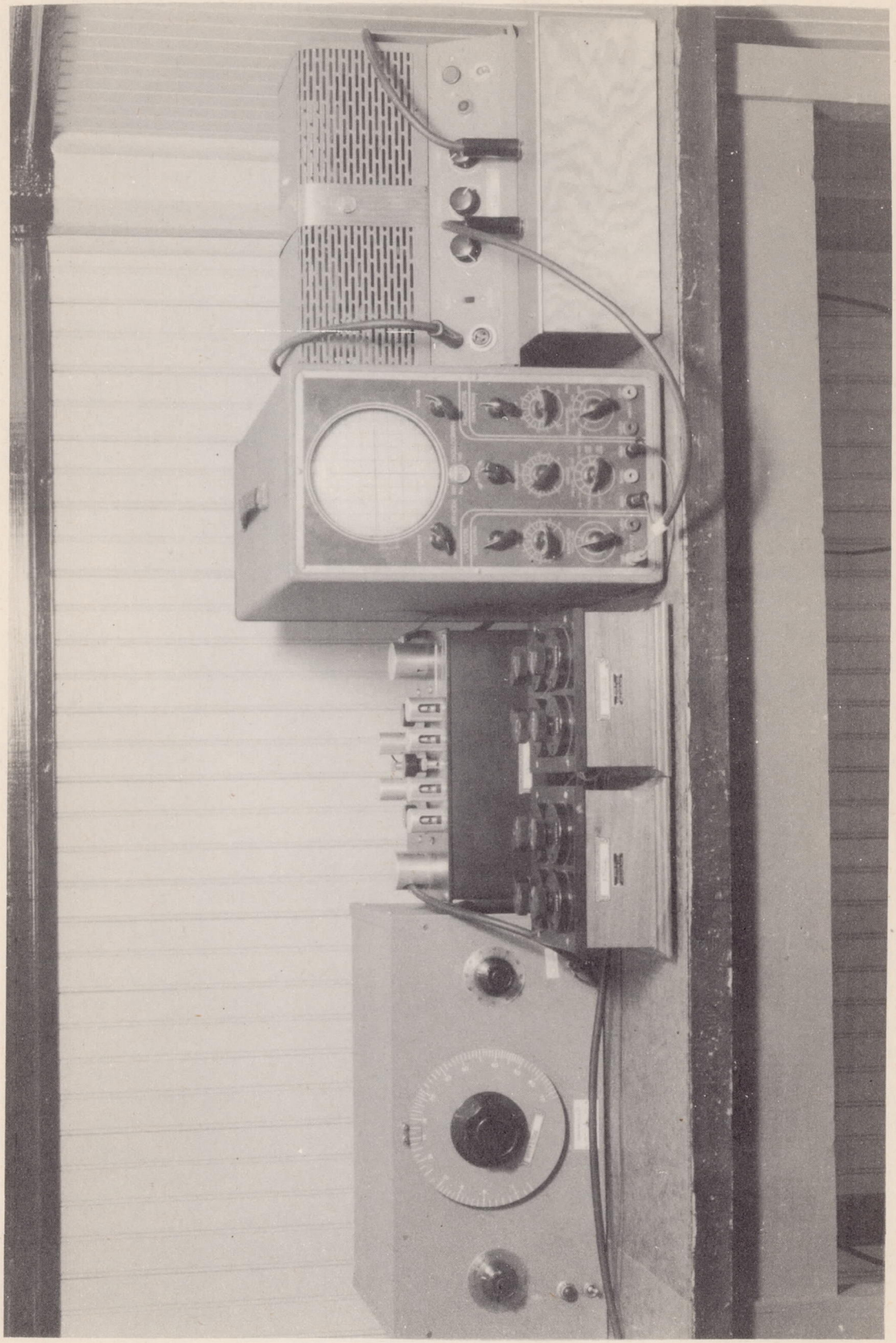

Fig. 3

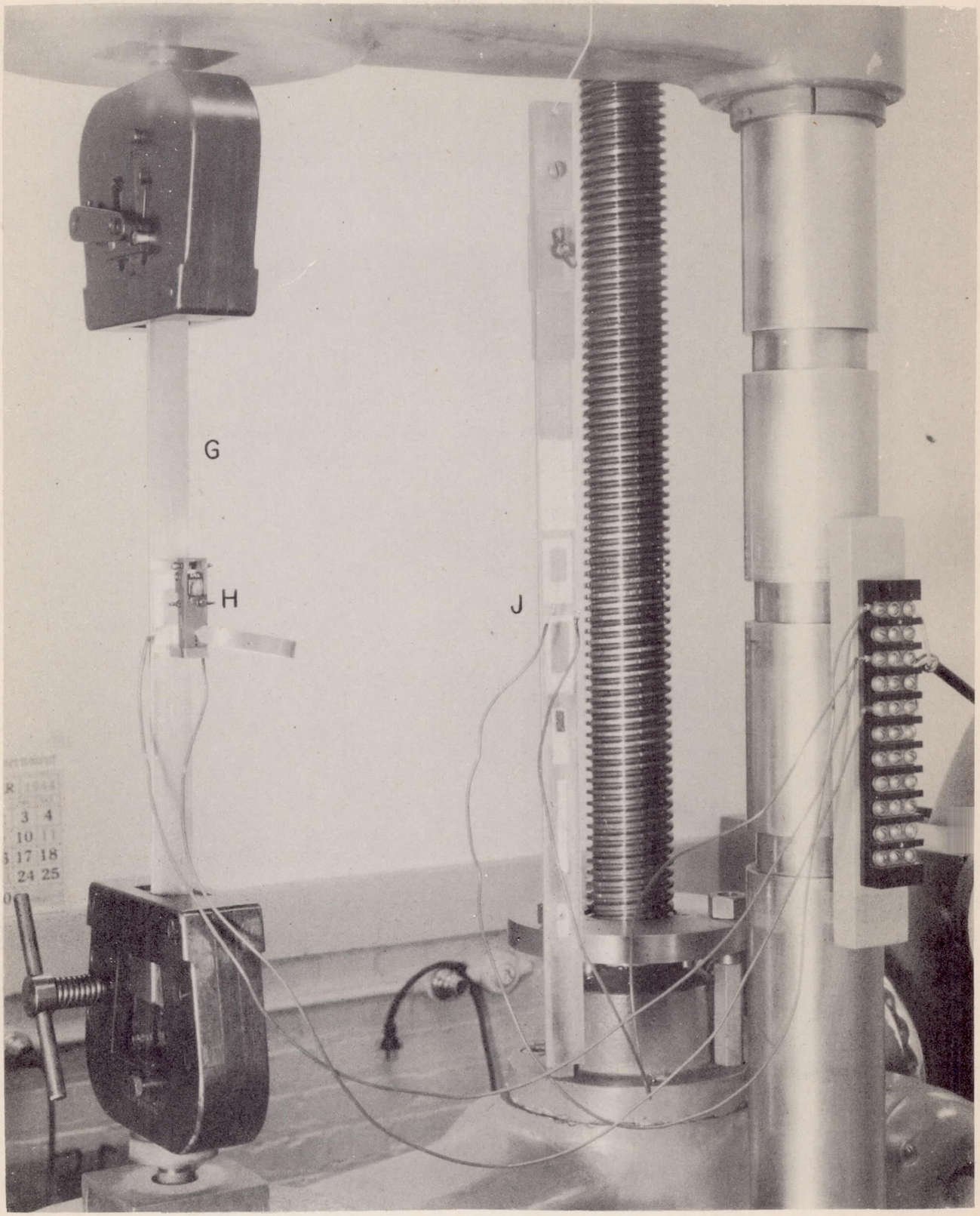

Fig. 4

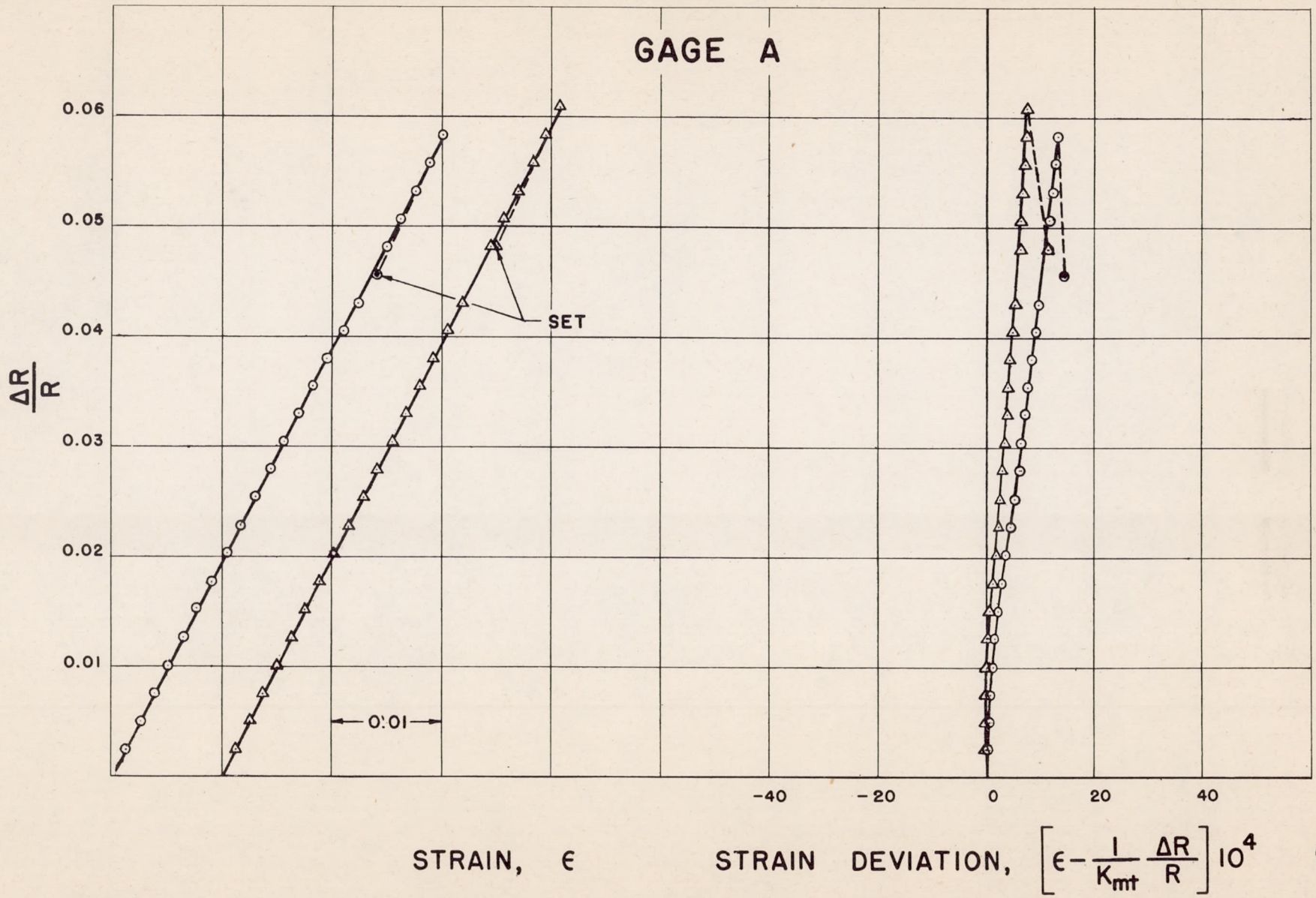
GAGE A
0.06
0.05
0.04
0.03
0.02
0.01
ΔR/R
SET
0.01
-40
-20
0
20
40
STRAIN, ϵ
STRAIN DEVIATION, [ϵ − 1/K_mt ΔR/R] 10^4

FIG. 5

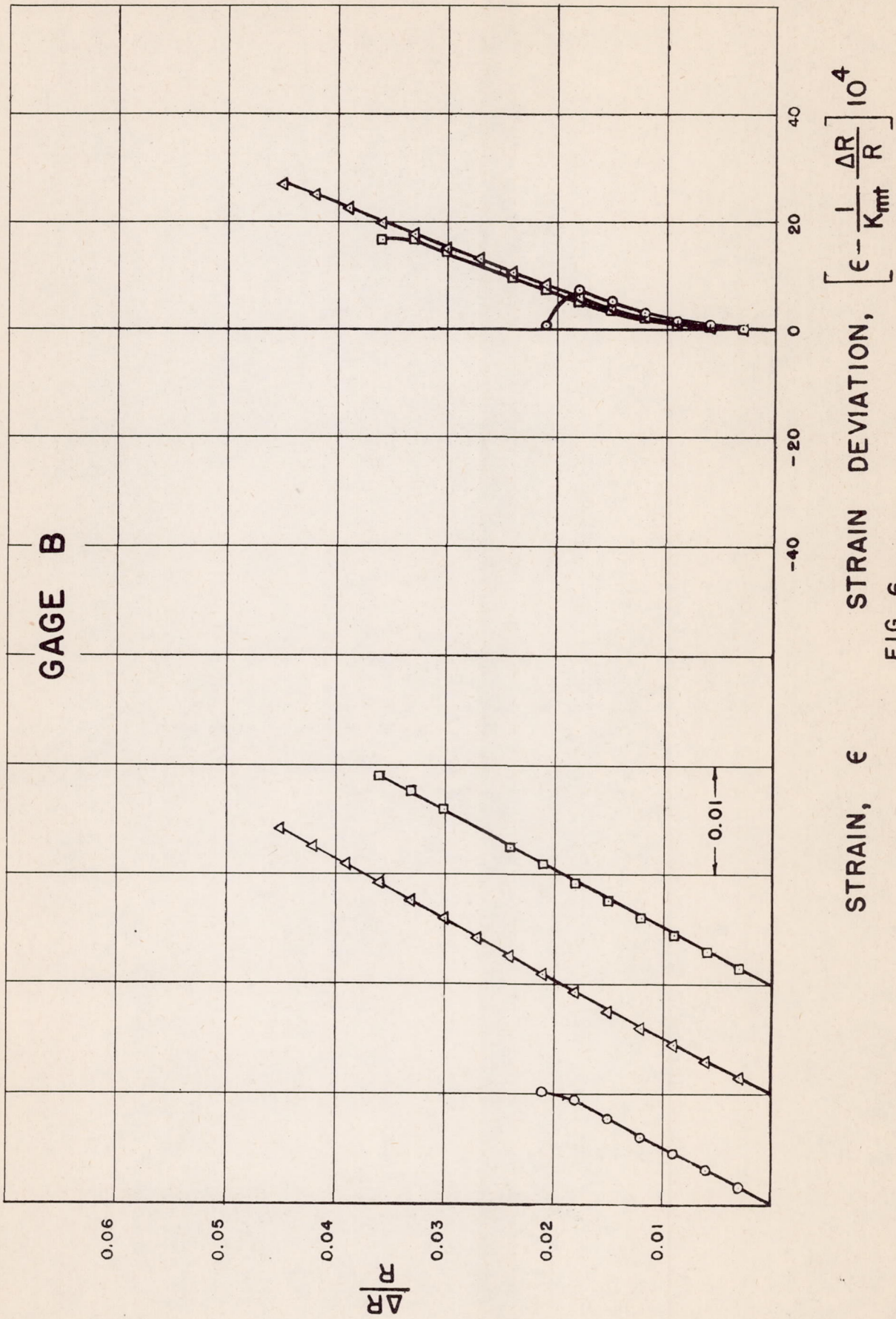
GAGE B
0.01
0.06
0.05
0.04
0.03
0.02
0.01
ΔR/R
40
20
0
-20
-40
STRAIN, ϵ
STRAIN DEVIATION, [ϵ - 1/K_mf (ΔR/R)] 10^4

FIG. 6

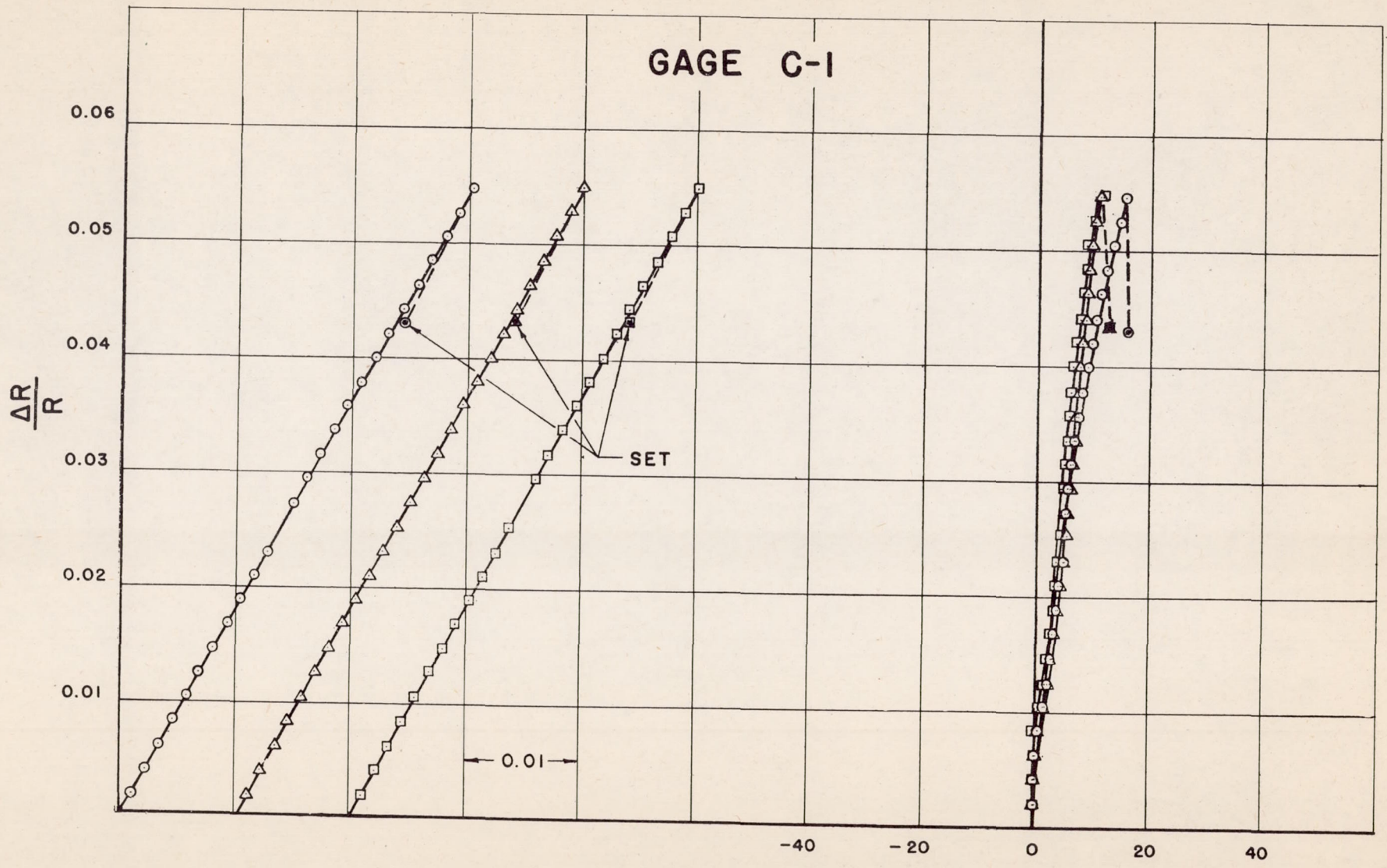
GAGE C-1
0.06
0.05
0.04
0.03
0.02
0.01
ΔR/R
SET
0.01
-40
-20
0
20
40
STRAIN, ϵ
STRAIN DEVIATION, [ϵ − 1/K_mt ΔR/R] 10^4

FIG. 7

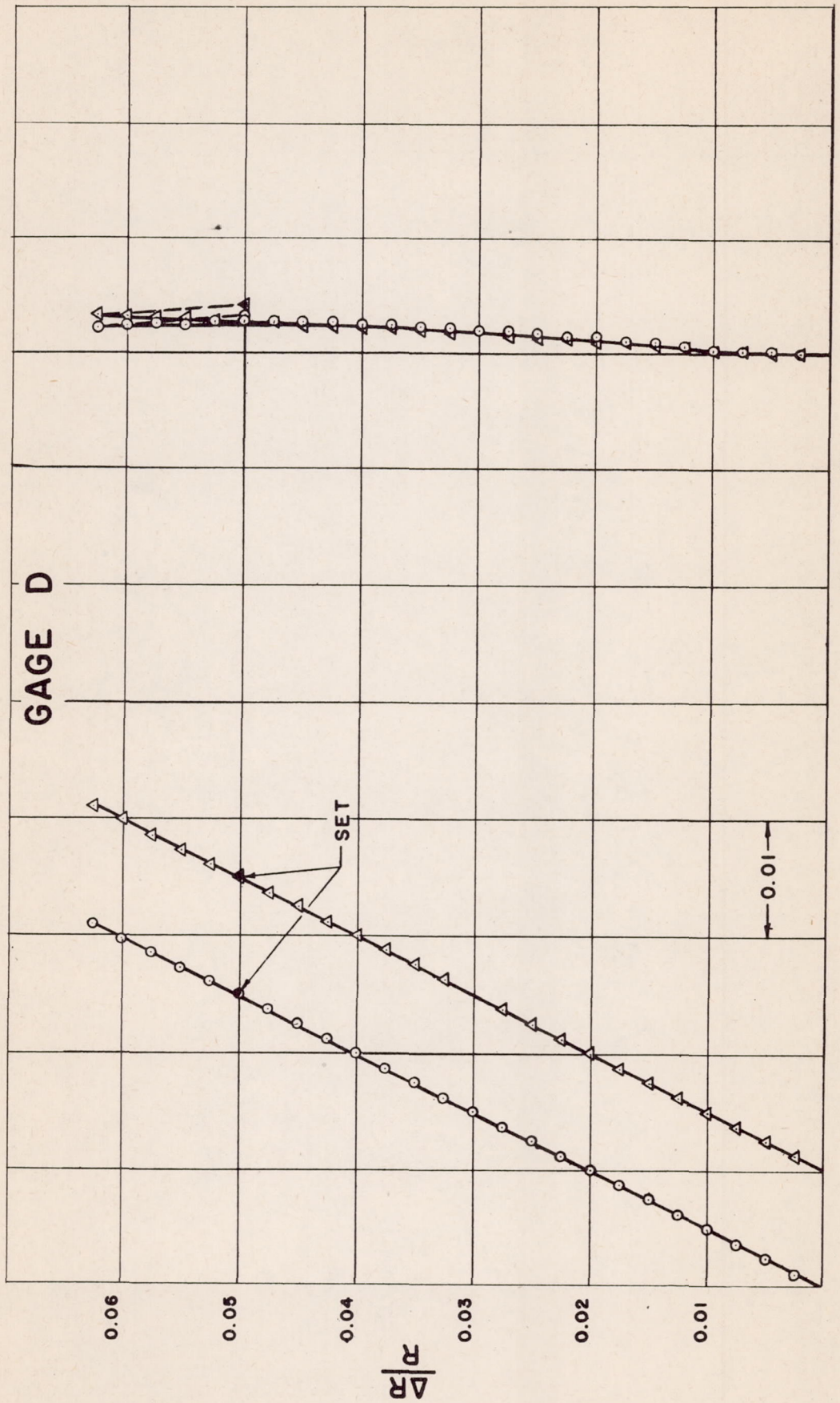
GAGE D
SET
0.01
0.06
0.05
0.04
0.03
0.02
0.01
ΔR/R
-40
-20
0
20
40
STRAIN, ϵ
STRAIN DEVIATION, [ϵ − 1/K_mf (ΔR/R)] 10^4

FIG. 8

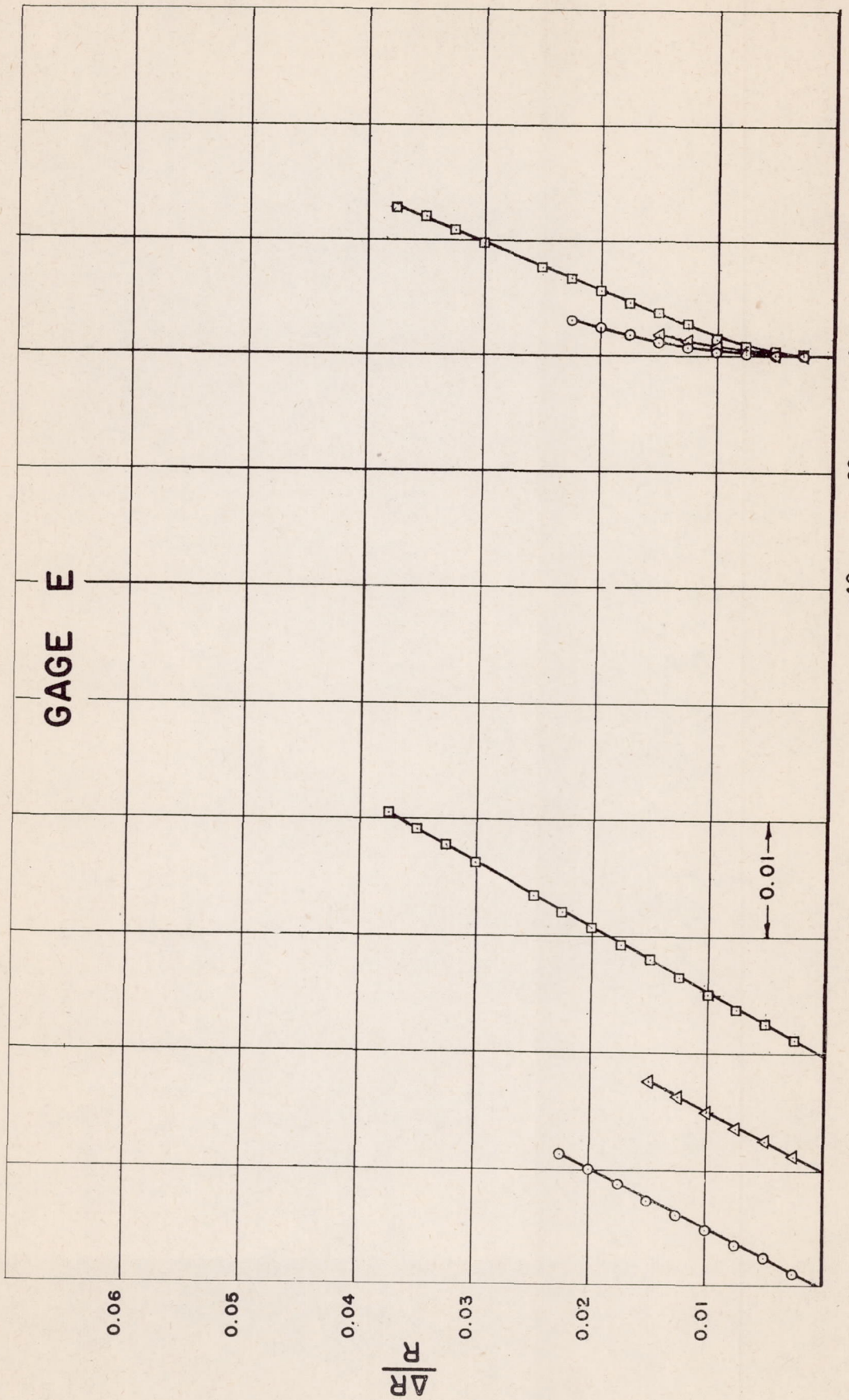
GAGE E
0.01
0.06
0.05
0.04
0.03
0.02
0.01
ΔR/R
40
20
0
-20
-40
STRAIN, ϵ
STRAIN DEVIATION, [ϵ − 1/K_mf (ΔR/R)] 10^4

FIG. 9

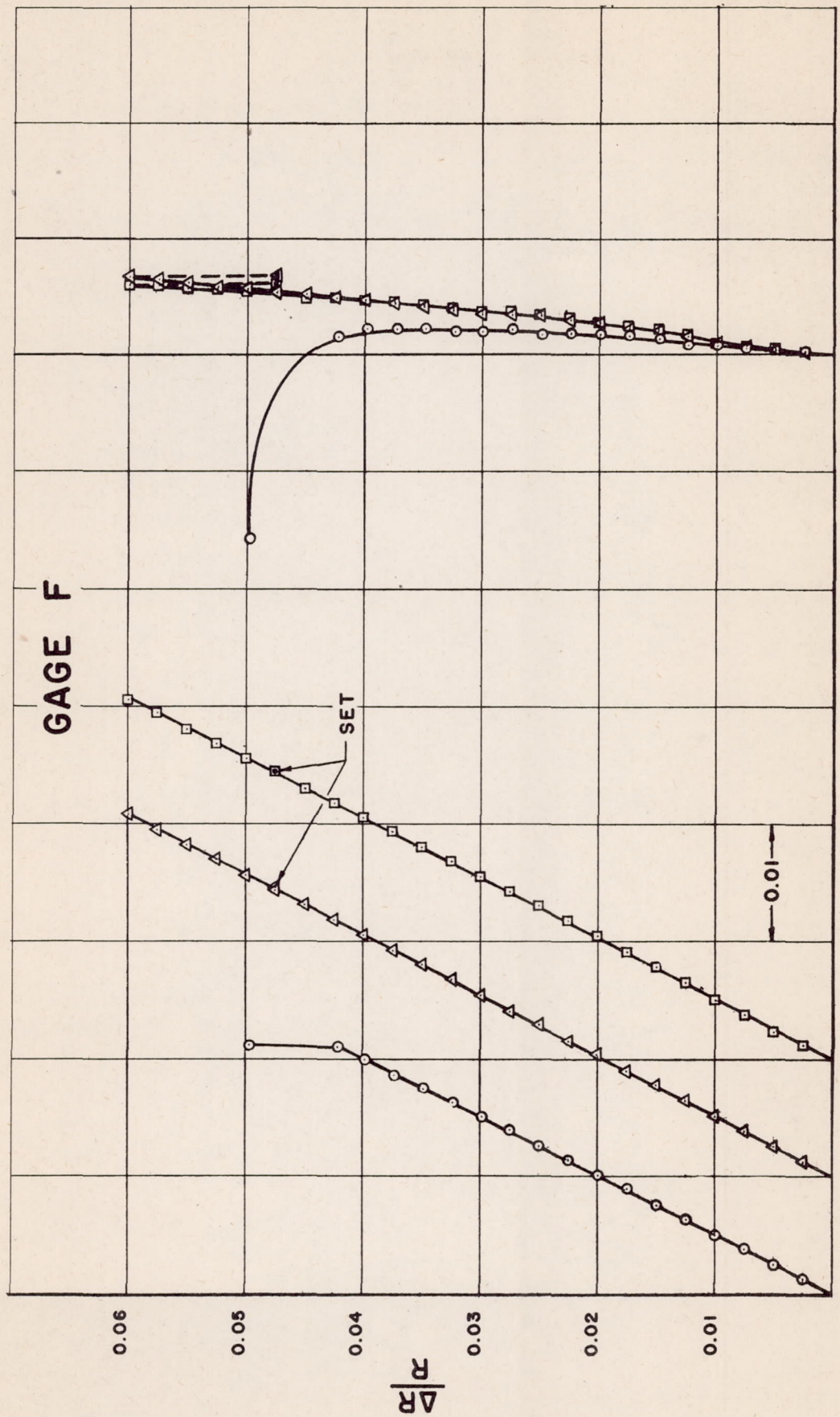
GAGE F
SET
0.01
0.06
0.05
0.04
0.03
0.02
0.01
ΔR/R
40
20
0
-20
-40
STRAIN DEVIATION, [ε − 1/K_mt (ΔR/R)] 10^4
STRAIN, ε

FIG. 10

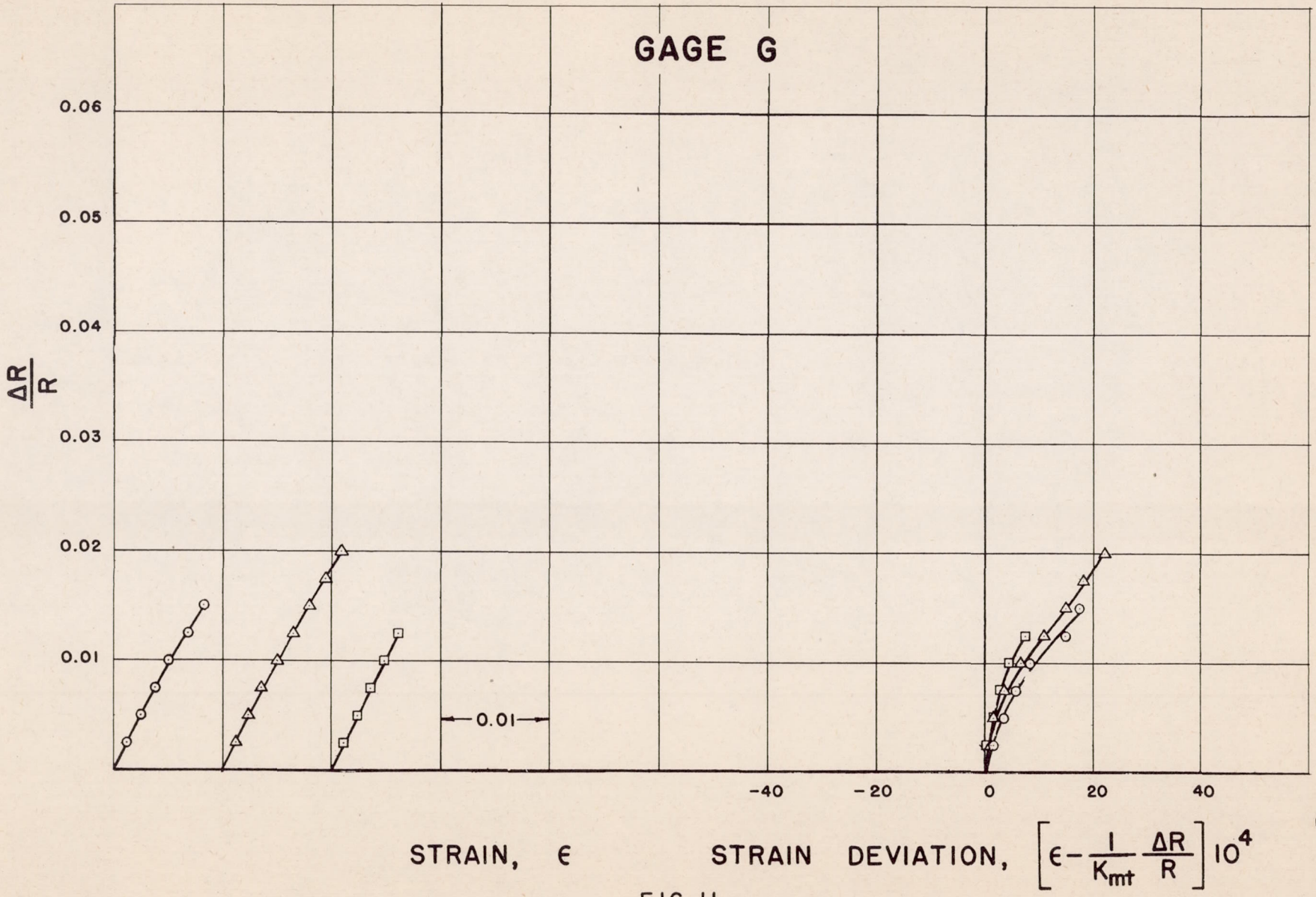
GAGE G
0.06
0.05
0.04
0.03
0.02
0.01
ΔR/R
0.01
-40
-20
0
20
40
STRAIN, ϵ
STRAIN DEVIATION, [ϵ − 1/K_mt ΔR/R] 10^4

FIG. 11

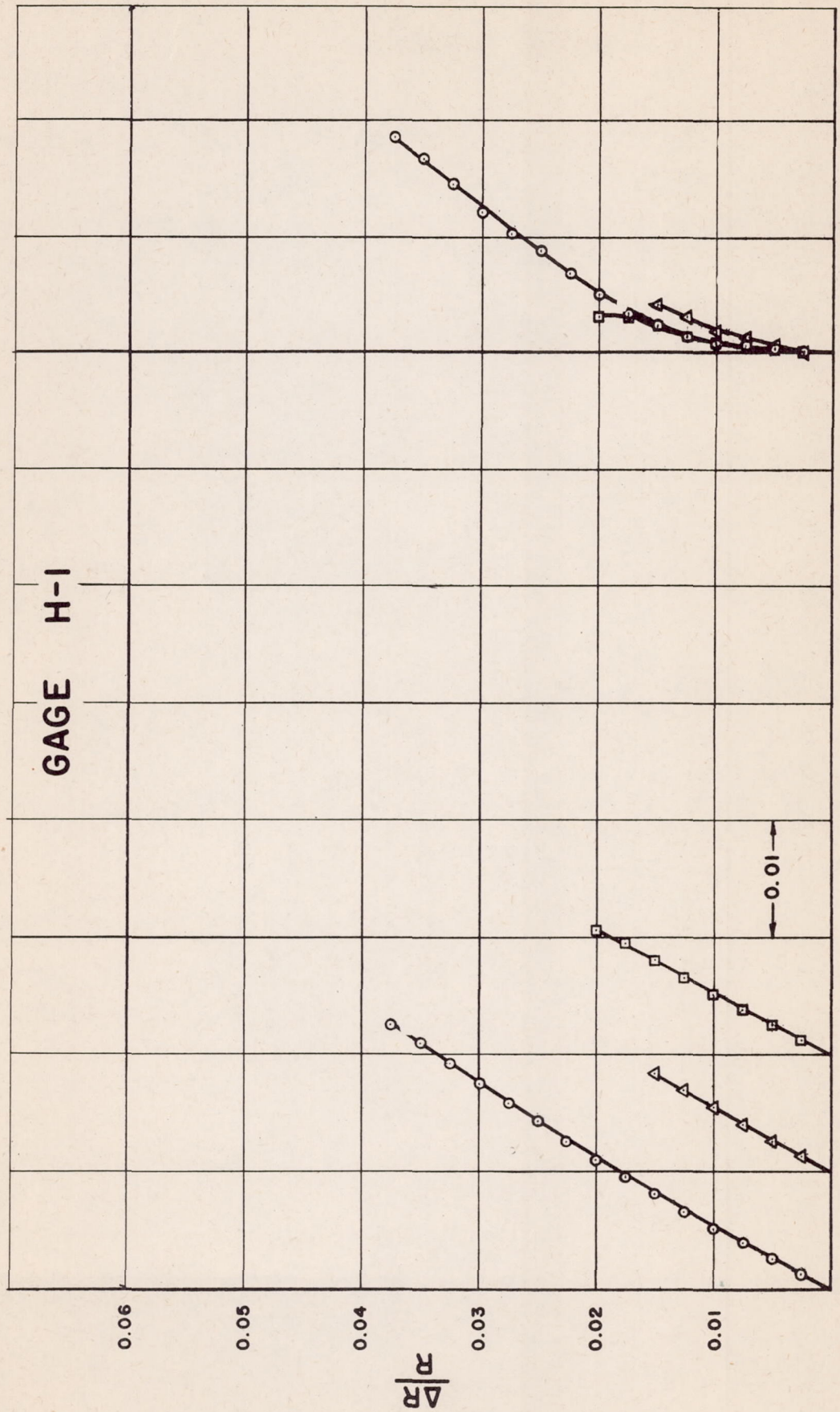
GAGE H-1
0.01
0.06
0.05
0.04
0.03
0.02
0.01
ΔR/R
-40
-20
0
20
40
STRAIN, ϵ
STRAIN DEVIATION, $\left[\epsilon - \frac{1}{K_{mf}} \frac{\Delta R}{R}\right] 10^4$

FIG. 12

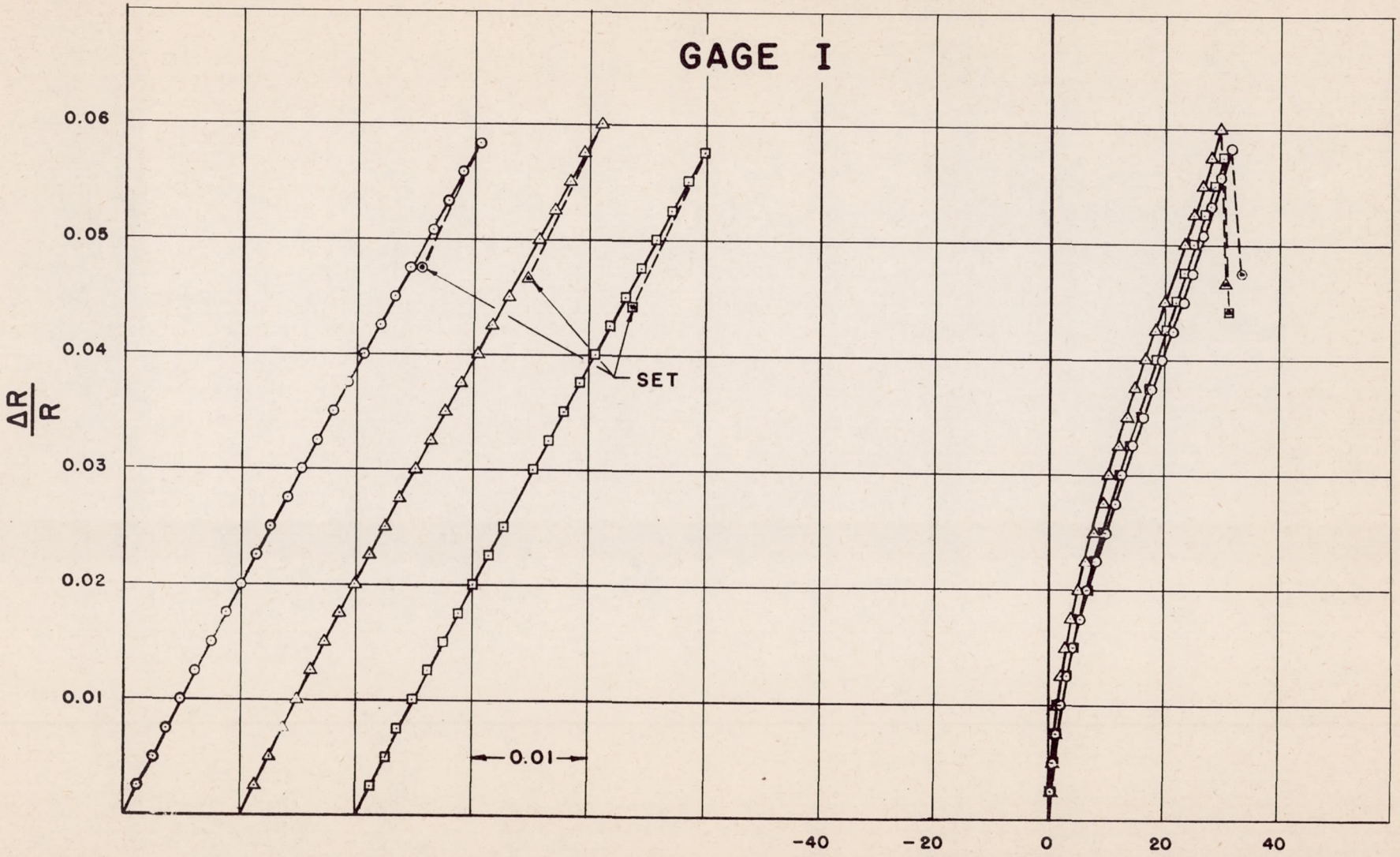
GAGE I
0.06
0.05
0.04
0.03
0.02
0.01
ΔR/R
SET
0.01
-40
-20
0
20
40
STRAIN, ϵ
STRAIN DEVIATION, [ϵ − 1/K_mt ΔR/R] 10^4

FIG. 13

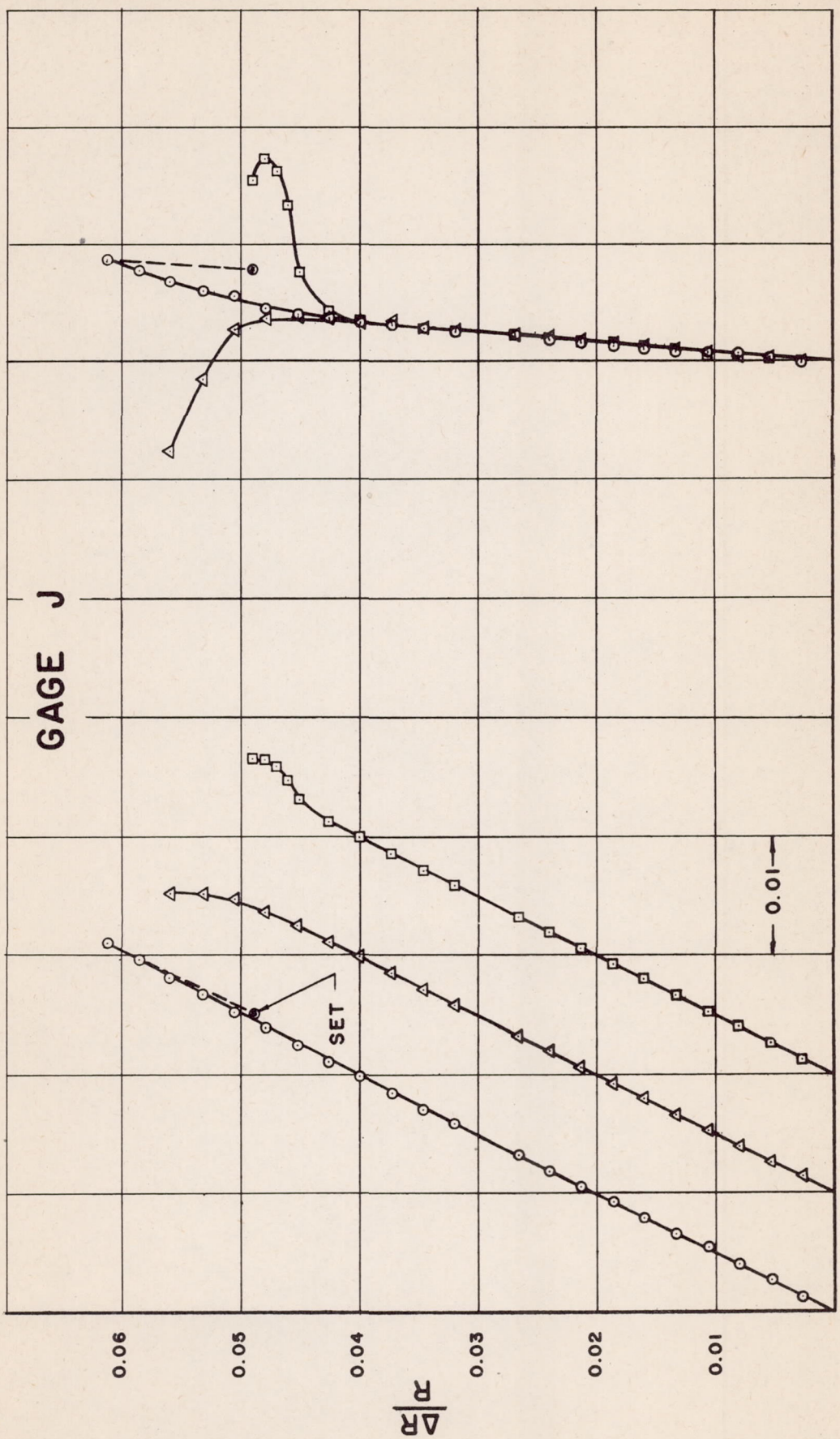
GAGE J
SET
0.01
0.06
0.05
0.04
0.03
0.02
0.01
ΔR/R
40
20
0
-20
-40
STRAIN, ϵ
STRAIN DEVIATION, $\left[\epsilon - \frac{1}{K_{mf}} \frac{\Delta R}{R}\right] 10^4$

FIG. 14

Fig. 15

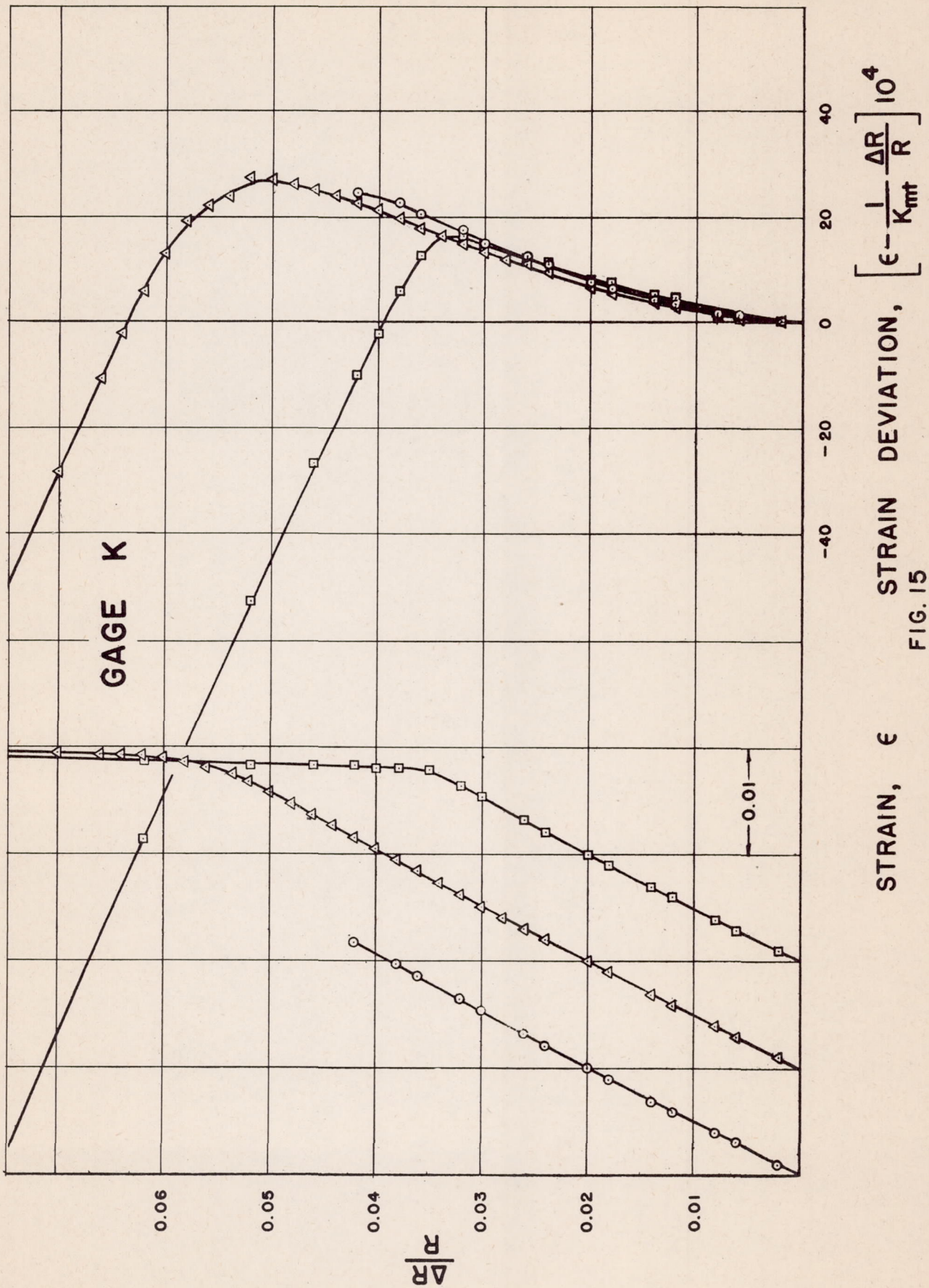
GAGE K
0.01
0.06
0.05
0.04
0.03
0.02
0.01
ΔR/R
40
20
0
-20
-40
STRAIN, ε
STRAIN DEVIATION, [ε - 1/K_mt (ΔR/R)] 10^4

FIG. 15

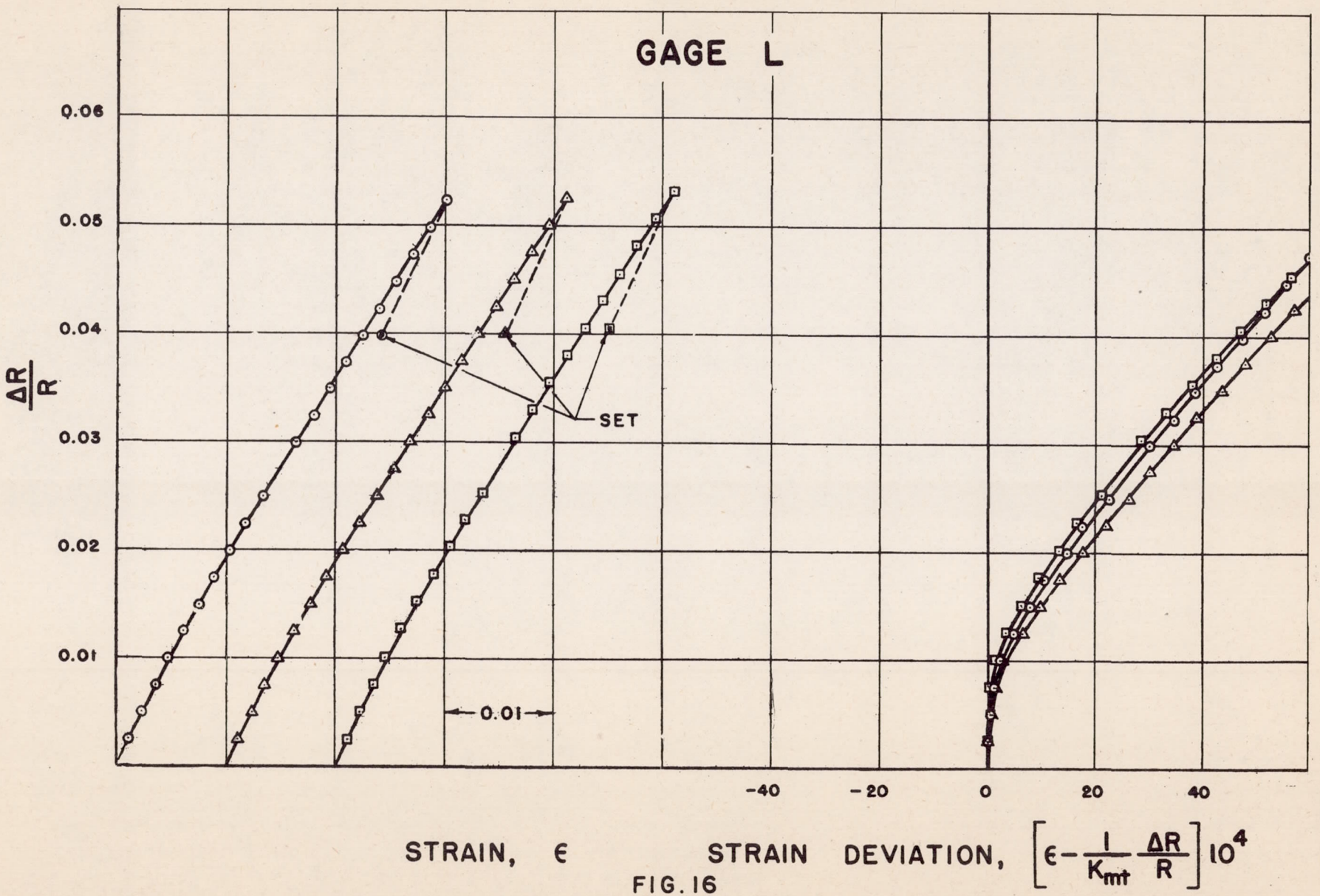
GAGE L
0.06
0.05
0.04
0.03
0.02
0.01
ΔR/R
SET
0.01
-40
-20
0
20
40
STRAIN, ϵ
STRAIN DEVIATION, [ϵ − 1/K_mt ΔR/R] 10^4

FIG. 16

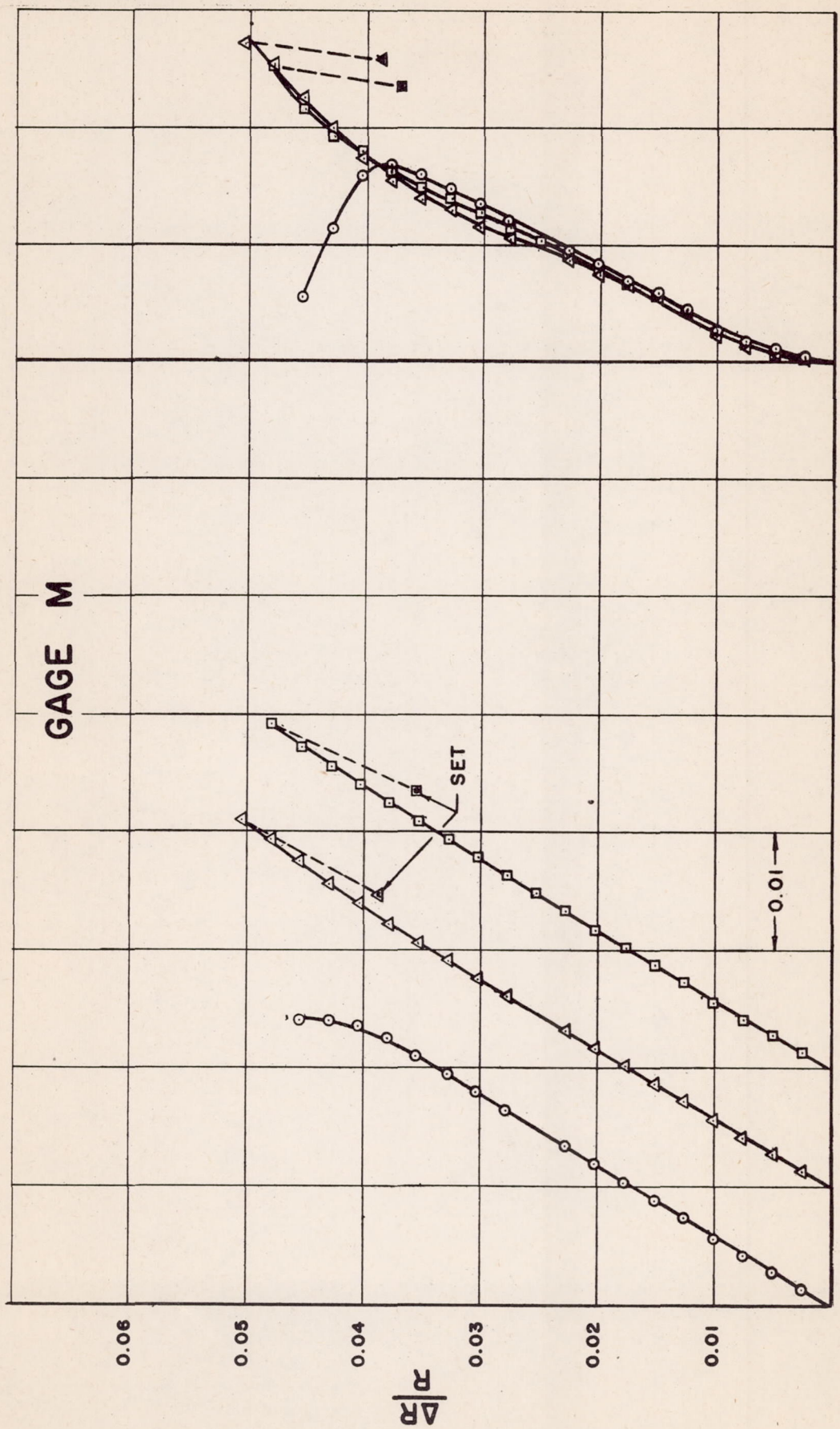
GAGE M
SET
0.01
0.06
0.05
0.04
0.03
0.02
0.01
ΔR/R
-40
-20
0
20
40
STRAIN, ϵ
STRAIN DEVIATION, [ϵ − 1/K_mf (ΔR/R)] 10^4

FIG. 17

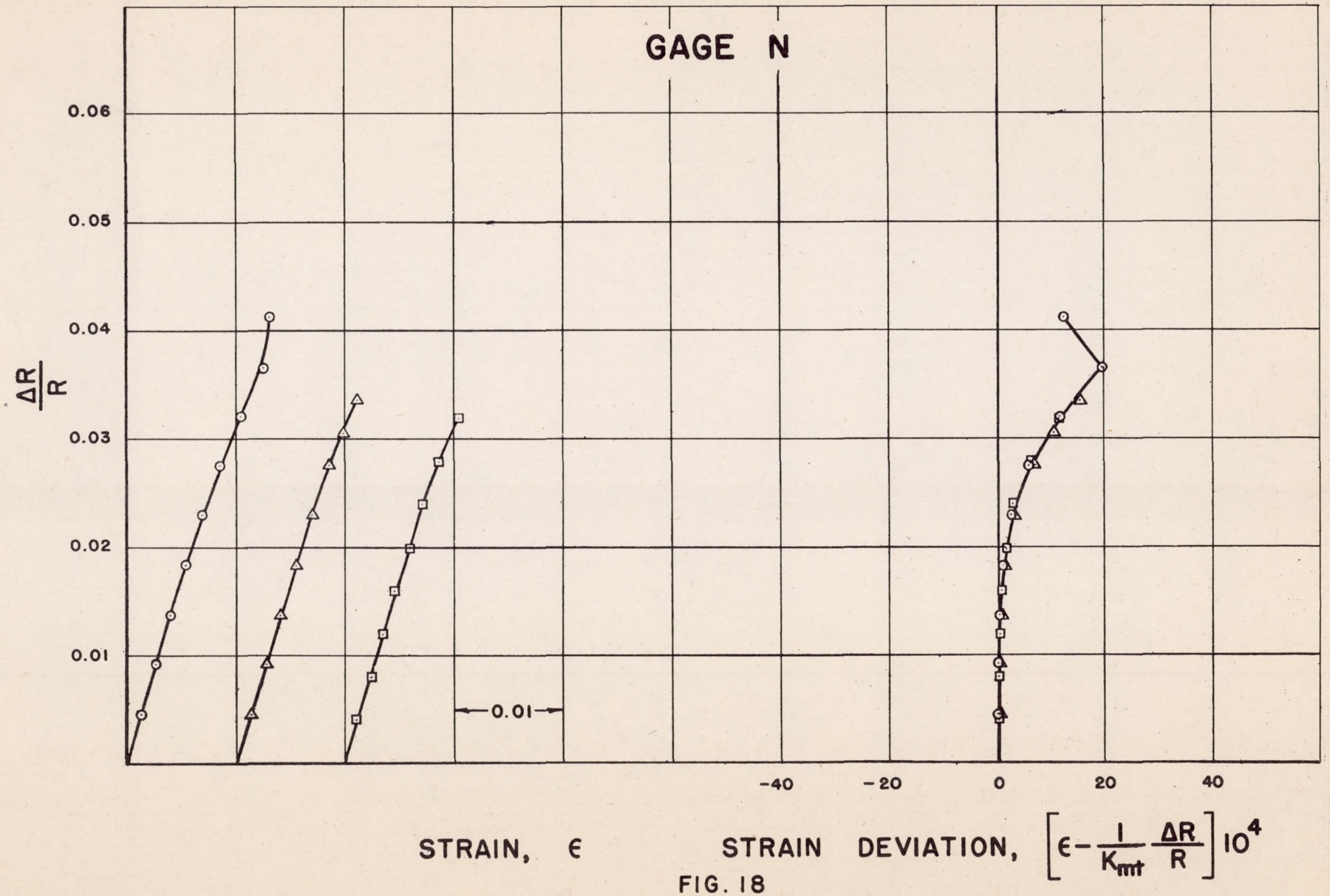
GAGE N
0.06
0.05
0.04
0.03
0.02
0.01
$\frac{\Delta R}{R}$
0.01
-40
-20
0
20
40
STRAIN, ϵ
STRAIN DEVIATION, $\left[\epsilon - \frac{1}{K_{mt}} \frac{\Delta R}{R}\right] 10^4$

FIG. 18

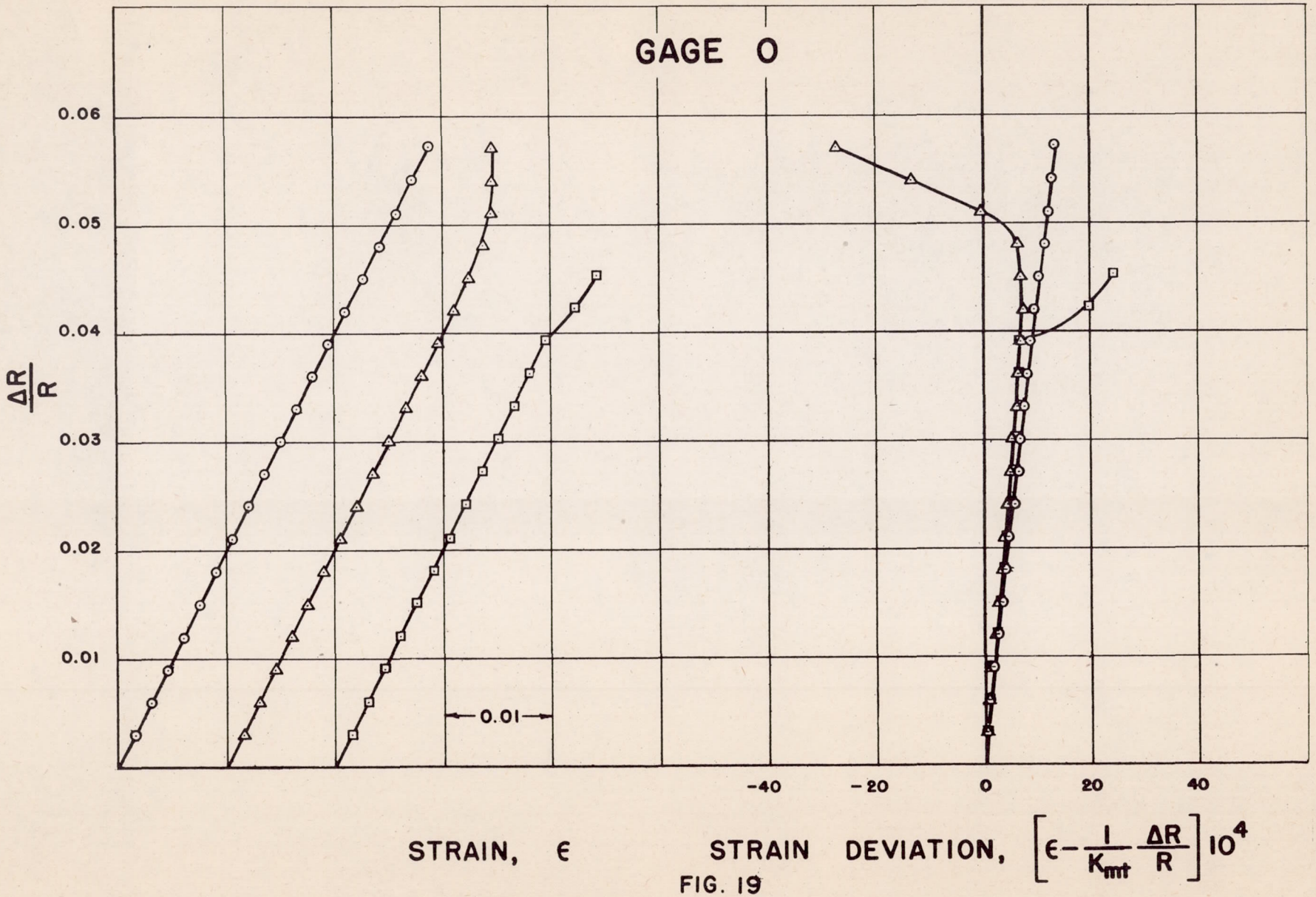
GAGE O
0.06
0.05
0.04
0.03
0.02
0.01
ΔR/R
0.01
-40
-20
0
20
40
STRAIN, ϵ
STRAIN DEVIATION, [ϵ − 1/K_mt ΔR/R] 10^4

FIG. 19

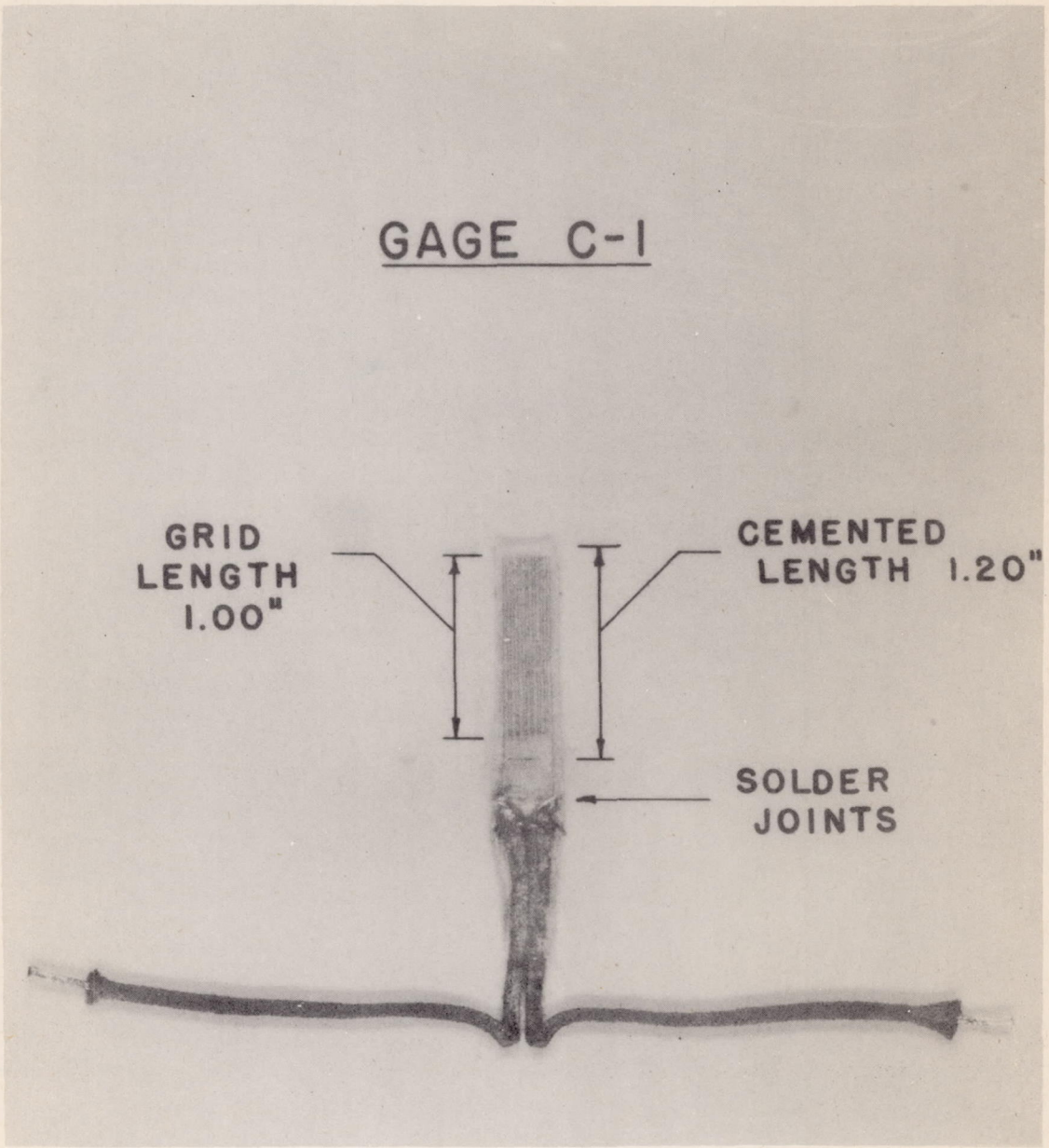

Fig. 20